SOx TRAPPING PERFORMANCES OF CuO BASED SILICA MESOPOROUS ADSORBENTS FOR DESULFURIZATION OF INDUSTRIAL FLUE GAS STREAM

Sophie Dorge, Université de Haute Alsace, France
sophie.dorge@uha.fr
Pierrick Gaudin, ersité de Haute Alsace, France
Marc Berger, Université de Haute Alsace ; ADEME - Agence de l'Environnement et de la Maîtrise de l'Energie, France
Habiba Nouali, ersité de Haute Alsace, France
Laure Michelin, ersité de Haute Alsace, France
Ludovic Josien, ersité de Haute Alsace, France
Matthieu Vierling, GE Energy, France
Michel Molière, Université de Technologie de Belfort-Montbéliard, France
Emmanuel Fiani, ADEME - Agence de l'Environnement et de la Maîtrise de l'Energie, France
David Habermacher, Université de Haute Alsace, France
Joël Patarin, ersité de Haute Alsace, France
Jean-François Brilhac, Université de Haute Alsace, France

KEY WORDS
SOx adsorbents, highly dispersed copper species, mesoporous silica support, SO_2 adsorption, multicycle experiments.

ABSTRACT
In the present work, CuO/SBA-15 SOx regenerable adsorbents were elaborated. Synthesis conditions were controlled in order to obtain highly dispersed Cu^{2+} species assumed to be Cu-O-Si species. Materials were evaluated as SOx adsorbents through multicycle adsorption/regeneration experiments. Their performances decrease along cycles due to copper species sintering and there is an optimal copper loading for a maximal SOx adsorption efficiency.

1. INTRODUCTION

Among the gaseous pollutants resulting from human activity, SOx (e.g. SO_2 + SO_3) are recognized both for their negative impact on the environment and their harmful effect on human health. More especially, they are one of the main precursors of secondary aerosols in the atmosphere (1). In order to minimize such effects, national emission ceilings have been set for SOx emissions at the international level through the Gothenburg Protocol and at the European level through the NEC (National Emission Ceilings) Directive 2001/81/EC. SOx emissions mainly originate from fossil fuel combustion, e.g. power generation plants. Consequently SOx emissions are stringently regulated through the IED (Industrial Emissions Directive) 2010/75/EU, with the obligation to achieve significant reduction rates by the use of technologies like Flue Gas Desulfurization (FGD) or fuel switch. Most of the present desulfurization processes consist in dry and wet scrubbing (2). Unfortunately, despite their proven efficiency, these processes suffer from high energy consumption and a non-regenerability which results in the production of large amounts of wastes ($CaSO_4$, Na_2SO_4…).
Therefore, the reversible SOx chemisorption on solid adsorbent emerged as an alternative to minimize environmental impact and energy costs. These adsorbents have to be able to 1) catalyze the oxidation of SO_2 to SO_3 (SO_2 + ½ O_2 → SO_3), 2) chemisorb SO_3 as metallic sulfates (x SO_3 + MOx → $M(SO_4)x$), 3) be regenerable ($M(SO_4)x$ → x SO_3 + MOx). Over the last decades, SOx trapping was investigated on a large variety of adsorbents such as oxides, mixed oxides, supported oxides, carbonaceous-based materials (2). Among these numerous studied materials, CuO/Al_2O_3 was reported as a promising solid for SOx trapping in the 300°C-500°C temperature range, that corresponds to the temperature existing in power stations (3). Such good performances are related to the high catalytic activity of CuO for the oxidation of SO_2 to SO_3 and the good SO_3 chemisorption as $CuSO_4$. Moreover, the regenerability of this material occurs at a moderate temperature (600°C) that keeps intact the morphological properties of the adsorbent and limits the energy consumption. Unfortunately, CuO/Al_2O_3 is limited since the support undergoes sulfation, both leading to aluminum sulfate species more difficult to decompose and to the modification of its textural properties that results in the decrease of the adsorbent lifetime.
In the present work, Organized Mesoporous Silica (OMS) SBA-15 supports were selected, firstly since SiO_2 was shown to be inert in regard with SOx. Moreover, the high specific surface area and porous volume of SBA-15

make them suitable for the incorporation of different elements such as metal oxides and allow an easy diffusion of SOx in the mesoporous channels. Given that the bulk sulfation of CuO is strongly kinetically limited (4), we aimed at develop a CuO/SBA-15 adsorbent exhibiting highly dispersed copper species. According to the literature, the dispersion of the heteroelement on the support depends on synthesis parameters (impregnation method, metal precursor, solvent used, nature of the support, drying step) and particularly on the calcination conditions (5). In order to get highly dispersed copper species on the SBA-15 support, the copper precursor (copper nitrate) was incorporated in SBA-15 by wet impregnation and the calcination step was performed under high synthetic air flow (6). The adsorbents' efficiency and stability for the SOx chemisorption reaction along multicycle operations was investigated during cycling experiments performed in fixed bed reactor. The adsorbents were fully characterized before and after SO_2 adsorption tests through nitrogen physisorption, X-Ray Diffraction (XRD), X-Ray Fluorescence (XRF), Scanning (SEM) and Transmission Electron Microscopy (TEM), to determine the evolution of the active phase (dispersion and crystalline nature) after experiments.

2. EXPERIMENTAL SECTION

2.1 Synthesis of SBA-15 mesoporous silica support

The SBA-15 mesoporous silica was synthesized as follows: 10.5 g of Pluronic 123 (Sigma-Aldrich) were dissolved in a solution containing 50 mL of HCl (37%, Sigma-Aldrich) and 330 mL of distilled water, at 55°C in a 500 mL beaker. After complete dissolution, 22.5 g of tetraethylorthosilicate (Sigma-Aldrich) were added and the solution was kept under stirring for 24 h at 55°C. The temperature was then raised up for 24 h for the synthesis step, until 90°C. The precipitate obtained was filtered, washed with distilled water and dried at 90°C overnight. The last step is a calcination at 300°C for 6 h under air with a temperature ramp of 1°C/min.

2.2 Preparation of the copper based adsorbents

The adsorbents were prepared as follows: the desired amount of $Cu(NO_3)_2.3H_2O$ (Sigma-Aldrich) was dissolved in 30 mL of distilled water in a 200 mL beaker. 2.0 g of support were added and the mixture was stirred at room temperature for 1 h. Then the beaker was introduced in an oil bath heated at 60°C, under stirring, until the water was completely evaporated. The powder was then dried overnight at 45°C. Then, it was calcined under air flow (60 NL/h) in a fixed-bed reactor (Ø = 15 mm, adsorbent bed thickness = 20 mm) at 500°C for 6 h with a ramp of 1°C/min.

2.3 SO_2 chemisorption tests and regeneration of the adsorbents

The SO_2 chemisorption tests were performed in a fixed bed reactor at 400°C, a temperature which corresponds to the conditions encountered in a gas turbine installation, using a gas mixture containing 250 ppm of SO_2 and 10 vol. % of O_2 diluted in nitrogen. The gas flow rate was equal to 13 NL/h and the Gas Hourly Space Velocity (GHSV) was chosen at 25000 h^{-1}, to be representative of gas turbine exhaust conditions. The SO_2 outlet concentration was continuously measured by an UV absorption analyzer. The dynamic SO_2 chemisorption capacity (C_{ads} expressed in moles of adsorbed SO_2 per gram of adsorbent) was calculated by integrating the SO_2 breakthrough curve until the SO_2 concentration at the outlet of the reactor reaches 75 ppm. This value was chosen since it is slightly lower than the SOx emission limit value currently enacted by the European regulation. The regeneration of the adsorbents (after each SO_2 chemisorption phase) was performed in situ, i.e. in the same experimental setup as the SO_2 chemisorption tests, under a nitrogen stream. The adsorbent was heated from 25 to 600°C at 5°C/min with a N_2 flow of 13 NL/h.

3. RESULTS AND DISCUSSION

In this work, three different copper loading were used: 8.8, 15.6 and 31.7 wt. % of CuO in the adsorbent. The three adsorbents were noted as CuO8.8/SBA-15, CuO15.6/SBA-15 and CuO31.7/SBA-15 respectively.

3.1 Characterization of the SBA-based adsorbents

The color of the fresh adsorbent with the lower copper content is light blue while it turns light green for higher copper loading (CuO15.6/SBA-15) and dark green for the fresh CuO31.7/SBA-15 sample. Given that crystalline copper oxide CuO is black, these colors suggest that copper species are not predominantly in the form of CuO but probably in strong interaction with the support, as discussed below (7).

The incorporation of copper in the SBA-15 material results in a decrease of the BET surface area of the material, from 825 m^2/g for the support SBA-15 (after calcination), to 459, 356 and 325 m^2/g for the CuO8.8/SBA-15, CuO15.6/SBA-15 and CuO31.7/SBA-15 samples, respectively (Table 1). The same trend is observed concerning the porous volumes which decrease from 1.02 cm^3/g to 0.65, 0.57 and 0.45 cm^3/g, respectively. Higher the copper loading, lower the BET surface area and porous volume. These decreases might be partly assigned to the densification of the mesoporous support due to the incorporation of copper and to a possible partial hydrolysis of the silica during the water evaporation step at 60°C. However, the low angle XRD analyses and N_2 physisorption isotherms clearly indicate that in all cases, the organized mesoporous structure of the support SBA-15 is preserved after the incorporation of copper. Indeed, all the adsorbents show type IV adsorption-desorption isotherms which correspond to organized mesoporous materials with well-ordered cylindrical pores (Figure 1). A shift of the capillary condensation zone toward lower pressure for the copper adsorbents traduces a decrease of the pore size after impregnation, from 6.8 nm for the support to 6.4, 6.3 and 6.1 nm for the CuO8.8/SBA-15, CuO15.6/SBA-15 and CuO31.7/SBA-15 samples, respectively.

Table 1: Chemical composition, textural properties of the three adsorbents.

Sample	Calcined SBA-15	CuO8.8/ SBA-15	CuO15.6/ SBA-15	CuO31.7/ SBA-15
Color	white	Light blue	Light green	Dark green
CuO content (wt. %)[a]	/	8.8	15.6	31.7
S_{BET} (m^2/g)	825	459	356	325
V_p (cm^3/g)	1.02	0.65	0.57	0.45
Pore size (nm)	6.8	6.4	6.3	6.1

[a] *Based on XRF characterizations*

All the active phase characterizations realized on the three different adsorbents (XRD, SEM and TEM analyses) clearly indicate the formation of copper species homogeneously dispersed on the support at the micrometric and nanometric scales.

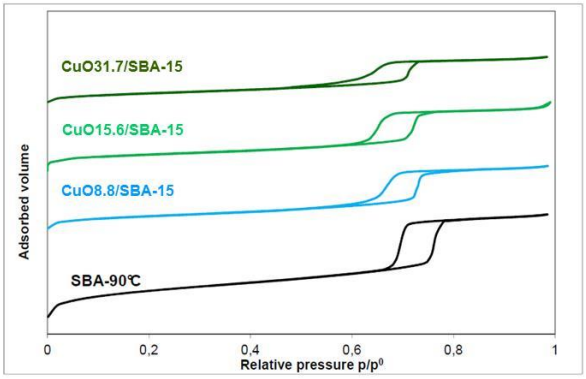

Figure 1: N_2 physisorption isotherms of the parent support and of the adsorbents. For a better visibility the isotherms are shifted along the Y axis.

Indeed, XRD analyses reveal no diffraction peak corresponding to a copper crystalline phase, indicating the presence of copper in strong interaction with the support, likely as Cu-O-Si species according to the literature (7,8), or amorphous particles. Moreover, the SEM (not presented here) and TEM micrographs Figure 2: A, C and E) of the three SBA-90-based adsorbents reported in figure 2 highlight the absence of CuO particles at the micrometric and nanometric scale, indicating a high dispersion of copper species.

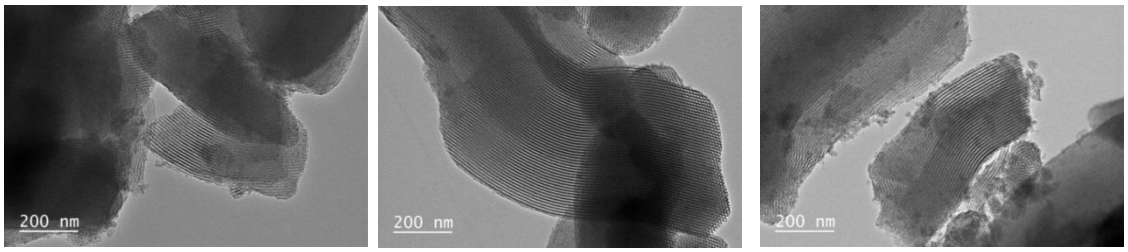

A B C

Figure 2: TEM micrographs (A, B and C) of the fresh adsorbents CuO8.8/SBA-15, CuO15.6/SBA-15 and CuO31.7/SBA-15 respectively.

3.2 SO_2 chemisorption measurements on the SBA-based adsorbents

The adsorbents were subjected to successive SO_2 chemisorption-regeneration tests in a fixed bed reactor. The SO_2 breakthrough curves obtained during multicycle experiments are reported in Figure 3. For each adsorption phase, the SO_2 adsorption capacities at 75 ppm (C_{ads}) and the Copper Sulfation Rate (CSR) were calculated, in order to evaluate the desulfurization efficiency of the copper species incorporated in the SBA-15 support. The SO_2 breakthrough curves of the CuO8.8/SBA-90 shows that the material is less efficient for the first SO_2 chemisorption (C_{ads} = 3.3x10^{-4} mol_{SO2}/g_{ads}, CSR = 29.7%) than for the following ones (C_{ads} ≥ 5.7x10^{-4} mol_{SO2}/g_{ads}, CSR ≥ 51.4%). Such a behavior is due to the thermal treatment at 600°C under N_2 flow for the regeneration which could lead to the reduction of Cu^{2+} to Cu^{+} species, more efficient in SO_2 trapping (9). For this adsorbent, no deactivation occurs, even after 9 chemisorption-regeneration cycles. On the contrary, the adsorbent efficiency increases progressively until the 9th cycle for which the SO_2 adsorption reaches 6.9x10^{-4} mol_{SO2}/g_{ads} (CSR=62.2%).

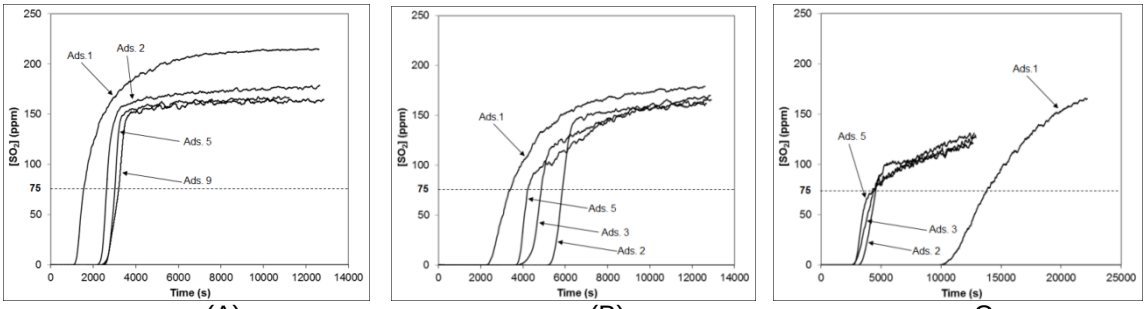

(A) (B) C

Figure 3: SO_2 breakthrough curves of the CuO8.8/SBA-15 (A), CuO15.6/SBA-15 (B) and CuO31.7/SBA-15 (C) adsorbents.

The performances of the CuO15.6/SBA-15 material is also more efficient during the second adsorption cycle (C_{ads} = 12.0x10^{-4} mol_{SO2}/g_{ads}, CSR = 61.2%) than during the first one (C_{ads} = 6.8x10^{-4} mol_{SO2}/g_{ads}, CSR = 34.7%) and after, slowly decrease until C_{ads} = 8.8x10^{-4} mol_{SO2}/g_{ads} (CSR = 44.9%) for the 5th cycle. Such a decrease is assigned to the sintering of copper species into bigger CuO particles, more difficult to be sulfated (4).
The CuO31.7/SBA-90 adsorbent (figure 3C) unambiguously behaves differently than the two others adsorbents. It exhibits a very high efficiency for the first SO_2 chemisorption with a C_{ads} equal to 25.4x10^{-4} $molS_{O2}/g_{ads}$ (CSR =

63.6%), due to the high content of incorporated copper. However this efficiency strongly decreases from the second SO_2 adsorption cycle and keeps decreasing until C_{ads} = 7.6x10^{-4} mol_{SO2}/g_{ads} (CSR = 19.0%) for the 5th cycle. As discussed below, this effect is assigned to the sintering of copper species into larger CuO particles. This decrease is more pronounced for the CuO31.7/SBA-90 adsorbent, due to its higher copper loading which favors the sintering effect.

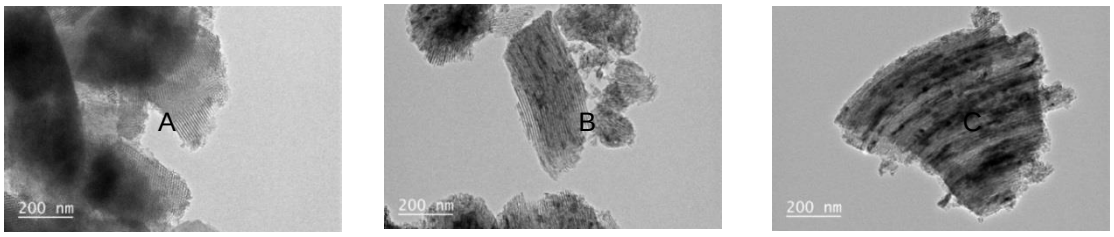

Figure 4: TEM micrographs (A, B and C) of the aged adsorbents (after SO_2 adsorption tests) CuO8.8/SBA-15, CuO15.6/SBA-15 and CuO31.7/SBA-15 respectively.

The XRD and TEM measurements of the adsorbents after cycling experiments clearly indicate the formation of CuO particles in the two adsorbents with the higher content of copper, whereas for the CuO8.8/SBA-15 material, no sintering of active phase is observed after SO_2 adsorption tests (Figure 4).

4. CONCLUSIONS

In this study, three copper silica based adsorbents were synthetized for the desulfurization of flue gas stream. The SO_2 adsorption multicycle experiments show that the adsorbent behavior strongly depends on the copper loading. For the lower copper loading (CuO8.8/SBA-90 sample) the adsorption capacity keeps slightly increasing from the 2nd to the 9th cycle. On the contrary, for the adsorbent with an intermediate copper loading (CuO15.6/SBA-15), a weak deactivation is observed, which is attributed to a slight sintering of copper species. For the highly copper loaded adsorbent (CuO31.7/SBA-15), its efficiency drops significantly early as the second cycle and then keeps slightly decreasing until the 5th cycle. Such a behavior is attributed to the high copper loading which results in the sintering of copper species in a significant extend into larger CuO particles. In summary, the CuO15.6/SBA-90 adsorbent appears as a good compromise since it shows both a sufficient SO_2 adsorption capacity (C_{ads} = 8.8x10^{-4} mol_{SO2}/g_{ads} for the 5th cycle) and a weak deactivation along multicycle operations. Moreover, the highly dispersed copper species appear to be more efficient than CuO particles for the desulfurization reaction.

ACKNOWLEDGMENT

This work (Project DeSOx New-Gen – contract #1281C0039) was supported by the French Agency for Environment and Energy Management (ADEME), through its funding program CORTEA.

REFERENCES

(1) A.P. Tsimpidi, V.A. Karydis, S.N. Pandis, J. Air Waste Manage. Assoc. 57 (2007) 1489-1498,
(2) Y. Mathieu, L. Tzanis, M. Soulard, J. Patarin, M. Vierling, M. Moliere, Fuel Process. Technol. 114 (2013) 81-100.
(3) G. Centi, S.Perathoner, Dev. Chem. Ens. Mineral Process. 8 (2000) 441-463.
(4) G. Centi, N. Passarini, S. Perathoner, A. Riva, Ind. Eng. Chem. Res. 31 (1992) 1947-1955.
(5) S.L. Soled, E. Iglesia, R.A. Fiato, J.E. Baumgartner, H. Vroman, S. Miseo, Top. Catal. 26 (2003) 101-109.
(6) P. Munnik, M. Wolters, A. Gabrielsson, S.D. Pollington, G. Headdock, J.H. Bitter, P.E. de Jongh, K.P. de Jong, J. Phys. Chem. C 115 (2011) 14698-14706.
(7) S.J. Gentry, P.T. Walsh, J. Chem. Soc. Faraday. Trans. 1 78 (1982) 1515-1523.
(8) X-C. Shao, L-H. Duan, Y-Y. Wu, Y-C. Qin, W-G. Yu, Y. Wang, H-L. Li, Z-L. Sun, L-J. Song, Acta Phys. Chim. Sin. 28 (2012) 1467-1473.
(9) M. Popova, A. Ristic, M. Mazaj, D. Maucec, M. Dimitrov, N. Novak Tusar, ChemCatChem. 6 (2014) 271-277.